AStA Advances in Statistical Analysis manuscript No.
(will be inserted by the editor)

Exact extreme value, product, and ratio distributions under non-standard assumptions

Klaus Müller · Wolf-Dieter Richter

Received: date / Accepted: date

Abstract The exact distributions of many functions of random vectors are derived in the literature mainly for the case of a Gaussian vector distribution or under the assumption that the vector follows a spherical or an elliptically contoured distribution. Numerous standard statistical applications are given for these cases. Deriving analogous results, if the sample distribution comes from a large family of probability laws, needs to make use of new analytical tools from the area of exact distribution theory. The present paper provides the application of such tools suitable for deriving the exact cumulative distribution functions and density functions of extreme values, products and ratios in $l_{2,p}$-symmetrically distributed populations. Accompanying simulation studies are presented in cases of power-exponentially distributed populations and for different sample sizes. As an application, well known results on the increasing failure rate properties of extremes from Gaussian samples are extended to p-power exponential sample distributions.

Keywords Geometric measure representation · $l_{2,p}$-generalized arc-length measure · intersection-percentage function · p-power exponential distribution · lifetime analysis · IFR property · simulation

1 Introduction

In lifetime analysis, one is interested in answering the question whether or not a statistic has an increasing failure rate (IFR). If one considers e.g. the max-

K. Müller
University of Rostock, Institute of Mathematics,
Ulmenstraße 69, Haus 3, 18057 Rostock, Germany
E-mail: klaus.mueller@uni-rostock.de

W.-D. Richter
University of Rostock, Institute of Mathematics,
Ulmenstraße 69, Haus 3, 18057 Rostock, Germany
E-mail: wolf-dieter.richter@uni-rostock.de

imum or the minimum statistic under the assumption that the sample vector follows a joint normal distribution, Gupta and Gupta (2001) give a positive reply. Answering the same question but in case that the sample distribution comes from a large class of multivariate probability laws needs to make use of new analytical tools from the area of exact distribution theory. The present paper provides the application of analytical tools suitable for deriving exact distributions of several statistics under certain non-standard assumptions and will particularly give an answer to the question asked above. Moreover, exact distributions will be compared with simulation results.

The exact distributions of functions of random vectors, like the arithmetical mean of the vector's components, i.e. the mean value statistic of a random sample, the student statistic, the empirical correlation coefficient, and many other statistics, were derived first in the case of a Gaussian vector distribution and later under the assumption that the vector follows a spherical or an elliptically contoured distribution. Numerous standard exact statistical distributions are derived for these cases, e.g., in Anderson (1984), Fang and Anderson (1990), Fang and Zhang (1990), and Gupta and Varga (1993). The present paper deals with exact distributions of extreme values, products, and ratios being special functions of certain types of random vectors.

Certain $l_{n,p}$-symmetric distributions have been studied in Schechtman and Zinn (1990), Rachev and Rüschendorf (1991), Gupta and Song (1997), Song and Gupta (1997), Szablowski (1998), and Richter (2009). It was shown in Hyvärinen (2007) and Sinz and Bethge (2008) that $l_{n,p}$-symmetric distributions fit natural image data better than the Gaussian one. The special case of the power-exponential distribution was introduced already in Subbotin (1923). Just like spherically and elliptically contoured distributions, the $l_{n,p}$-symmetric distributions allow modelling of both heavy and light tails. This circumstance can be of special interest, e.g., in insurance and financial mathematics as well as in reliability theory and many other fields. For some basics on heavy and light tails and several applications, we refer to Adler et al (1998), Vázquez et al (2006), Balkema and Embrechts (2007), and Tang (2008). Exact distributions of certain statistic in $l_{n,p}$-symmetrically distributed populations were studied for special cases in Harter (1951), Press (1969), Arnold and Brockett (1992), Nadarajah (2005a,b), Nadarajah and Gupta (2005), Nadarajah and Kotz (2005), and Kalke et al (2013), and for some general cases in Arellano-Valle and Richter (2012) and Günzel et al (2012). Basics on geometric disintegration and on deriving exact distributions under non-standard model assumptions are discussed in Richter (2012).

The aim of the present paper is to derive the cumulative distribution function (cdf) and the probability density function (pdf) for the extreme values, products, and ratios of the components of $l_{2,p}$-symmetrically distributed random vectors with arbitrary $p > 0$ and arbitrary density generating function (dgf). Furthermore, we will compare the exact results with those generated by simulation studies of different sample sizes. Finally, we will consider the IFR property for extreme statistics in the case of $l_{2,p}$-sample distributions.

A function $g\colon [0,\infty) \to [0,\infty)$ is called a dgf of an $l_{2,p}$-symmetric probability distribution if it satisfies the inequalities

$$0 < \int_0^\infty r g(r^p)\, dr < \infty.$$

A two-dimensional random vector $X = (X_1, X_2)$ with a density

$$\varphi_{g,p}(x) = C_{2,g,p}\, g\left(|x|_p^p\right), \quad x \in \mathbb{R}^2$$

is said to follow the $l_{2,p}$-symmetric distribution $\Phi_{g,p}$. Here, the p-functional

$$|x|_p = \left(|x_1|^p + |x_2|^p\right)^{\frac{1}{p}}, \quad x = (x_1, x_2) \in \mathbb{R}^2$$

denotes the $l_{2,p}$-norm if $p \geq 1$ and, according to Moszyńska and Richter (2012), an antinorm if $p \in (0,1)$, and $C_{2,g,p}$ is a normalizing constant such that

$$\int_{\mathbb{R}^2} \varphi_{g,p}(x)\, dx = 1.$$

For more details concerning the normalizing constants and examples of density generating functions and their generated distributions, we refer to Kalke et al (2013).

An important subclass of the $l_{2,p}$-symmetric distribution class is the class of power-exponential distributions. Several analytical questions like, e.g., the determination of the normalizing constant or that of moments are easier to deal with within this subclass than for certain other elements from the general class of $l_{2,p}$-symmetric distributions. Moreover, figures of densities of such distributions may be easily drawn exactly for elements from the subclass whereas the general case needs additional assumptions and calculations concerning the dgf and the corresponding normalizing constant, respectively. Nevertheless, one may consider figures of these special densities as reflecting general properties being true in the whole class of $l_{2,p}$-symmetric distributions. Further, notice that power-exponentially distributed random vectors have stochastically independent components which is not the case outside this subclass. As a consequence, any simulations are easier to be done if random vectors follow a distribution from within the subclass of power-exponential distributions than from outside of it. Finally, we mention that p-power exponential distributions with $p \in (0,1)$ are limiting distributions in certain sampling schemes. For details, we refer to Steutel and van Harn (2004), Richter (2007), and Kalke (2013).

To be more concrete, a two-dimensional random vector is said to follow a power-exponential (or the p-generalized Gaussian or Laplace) distribution with parameter $p > 0$ and independent components if it has the density

$$f_p(x) = \left(\frac{p^{1-\frac{1}{p}}}{2\Gamma\left(\frac{1}{p}\right)}\right)^2 \exp\left\{-\frac{|x_1|^p + |x_2|^p}{p}\right\}, \quad x = (x_1, x_2) \in \mathbb{R}^2.$$

This distribution was introduced in Subbotin (1923) and corresponds to the dgf $g_p(c) = \exp\left(-\frac{c}{p}\right)$, $c \in (0, \infty)$. The densities f_p are illustrated in Figure 1.1 and their $\left(\left(\frac{p^{1-\frac{1}{p}}}{2\Gamma\left(\frac{1}{p}\right)}\right)^2 e^{-\frac{1}{p}}\right)$-level sets for several parameters $p > 0$ in Figure 1.2 (figures are drawn throughout this paper using GeoGebra or several R or Matlab routines). The a-level sets of the density f_p, $\left\{x \in \mathbb{R}^2 \colon f_p(x) = a\right\} \subset \mathbb{R}^2$, $a > 0$, are actually the $l_{2,p}$-circles $S_{2,p}(r) = \left\{x \in \mathbb{R}^2 \colon |x|_p = r\right\}$ of suitably chosen p-radius $r > 0$ and with center $0 \in \mathbb{R}^2$. The notion of a p-generalized radius is motivated by the circumstance that circles $S_{2,p}(r)$ satisfy the representation $S_{2,p}(r) = r \cdot S_{2,p}$ with $S_{2,p} = S_{2,p}(1)$. The level sets of general $l_{2,p}$-symmetric densities are always $l_{2,p}$-circles having radii depending on the dgf g. For the graphs of the one-dimensional marginal densities of the p-generalized Gaussian distribution, we refer to Figure 1.3.

The distribution $\Phi_{g_p,p}$ is well-known as Laplace distribution if $p = 1$, Gaussian distribution if $p = 2$ and continuous uniform distribution on $(-1, 1)^{\times 2}$ in the limit case $p \to \infty$.

The rest of the paper is organized as follows. In Section 2, the general method of how to gain exact representations of functions of $l_{2,p}$-symmetrically distributed random vectors will be introduced. This method is used in Section

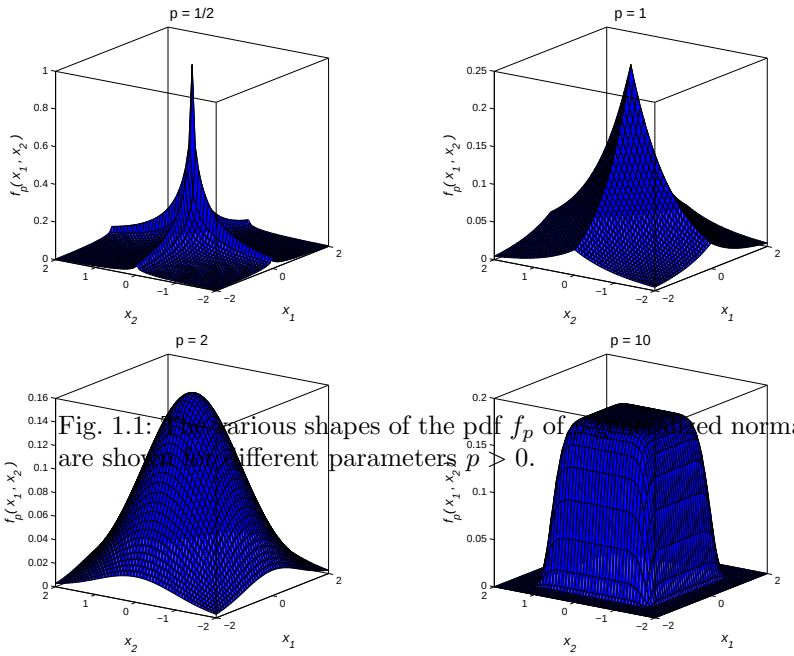

Fig. 1.1: The various shapes of the pdf f_p of the generalized normal distribution are shown for different parameters $p > 0$.

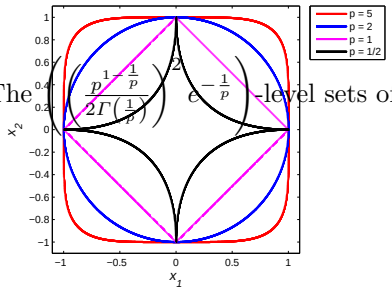

Fig. 1.2: The f_p-level sets of f_p are $l_{2,p}$-unit circles $S_{2,p}$.

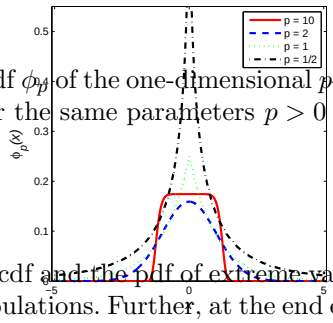

Fig. 1.3: The pdf ϕ_p of the one-dimensional p-generalized Gaussian distribution is visualized for the same parameters $p > 0$ as in Figure 1.1.

3 to derive the cdf and the pdf of extreme-value statistics of $l_{2,p}$-symmetrically distributed populations. Further, at the end of Section 3, we present simulation results for the cdf and the pdf of the maximum statistic in cases of small and large sample sizes. To this end, we shall use the R-module 'pgnorm' which has arisen from Kalke and Richter (2013). In Sections 4 and 5, we follow the line of Section 3 and get the cdf and the pdf of the product and the ratio of the components of $l_{2,p}$-symmetrically distributed random vectors, but their derivations will not be given as detailed as there. For better orientation, we will use various symbols for the different statistics studied in Sections 3, 4, and 5. Afterwards, we consider the IFR property for extreme value statistics. In the final Section 7, we draw some conclusions from our work done in this paper.

2 General method for deriving exact distributions

The method, used in this note to determine exact distributions of certain functions of a random vector under non-standard assumptions concerning the distribution of the random vector itself, may be simultaneously viewed under different aspects. The aspects of geometric measure representations and stochastic representations of corresponding random vectors are emphasized, e.g., in Richter (2009, 2013). The aspect of dealing with scale mixtures of p-generalized normal distributions was discussed in some detail in Arellano-Valle and Richter (2012), Section 3.3. Roughly spoken, $l_{2,p}$-symmetric distributions may be written under this point of view as scale mixtures of p-generalized uniform distributions on $l_{2,p}$-circles. This allows to compute the mass of a set A by computing intersections of normalized sets with the $l_{2,p}$-unit circle. The aspect of a non-Euclidian generalization of the classical method of indivisibles was discussed to some extent, e.g., in Richter (2012). All these points of view are closely connected with the method of disintegration and that of using conditional distributions which are well established in mathematical and statistical literature and will be considered under some geometric aspect in Richter (2014a,b), and under rather general assumptions upon the vector distribution.

In this paper, the actual main idea of how to derive the exact representations of the cdf of the extreme values, the product and the ratio of the components of $X \sim \Phi_{g,p}$ can be considered as to start from a geometric measure representation formula for continuous $l_{2,p}$-symmetric distributions which follows from Richter (2009). The following function $\mathfrak{F}_p \colon (0,\infty) \to [0,\infty)$ is basic for this geometric representation of $\Phi_{g,p}$. It is defined by

$$r \mapsto \mathfrak{F}_p(A,r) = \frac{AL_{p,q}\left([r^{-1}A] \cap S_{2,p}\right)}{AL_{p,q}(S_{2,p})}$$

and will be called the $l_{2,p}$-circle intersection-percentage function (ipf) of the set $A \in \mathfrak{B}^2$, according to Richter (2007). Here, $AL_{p,q}(M)$ denotes the $l_{2,q}$-arc-length of the Borel subset M of $S_{2,p}$ with $\frac{1}{p}+\frac{1}{q}=1$ which is defined as the limiting value of sums of length of polygons. For technical details concerning this non-Euclidian arc-length measure, we refer to Richter (2007, 2008a,b, 2009). Using the notation ω_p for the p-generalized uniform distribution on the $l_{2,p}$-unit circle $S_{2,p}$, it was said in these papers that $\mathfrak{F}_p(A,r) = \omega_p\left([r^{-1}A] \cap S_{2,p}\right)$. As first examples, the ipf of cones or double cones with vertex in the origin and a non-empty interior are positve constants that are less than or equal to 1. Such constants depend on the argument of the cdf of a p-generalized Student- or Fisher-statistic, respectively, and are calculated in Richter (2007, 2009) where p-generalized Student- and Fisher-distributions are derived, respectively. As a further example, one can consider the $l_{2,p}$-disc $K_{2,p}(\rho) = \left\{x \in \mathbb{R}^2 \colon |x|_p \le \rho\right\}$ with the center $0 \in \mathbb{R}^2$ and the p-radius $\rho > 0$. Then, $\mathfrak{F}_p(K_{2,p}(\rho), r) = I_{(0,\rho]}(r)$. This result leads immediately to a p-generalization of the χ^2-distribution as was shown in Richter (2007).

According to Richter (2009), for arbitrary $p > 0$, the $l_{2,p}$-symmetric distribution with dgf g satisfies the geometric measure representation

$$\Phi_{g,p}(A) = \frac{1}{I_{2,g,p}} \int_0^\infty \mathfrak{F}_p(A,r)\, rg\left(r^p\right)\, dr, \quad A \in \mathfrak{B}^2, \tag{2.1}$$

with $I_{2,g,p} = \int_0^\infty rg\left(r^p\right)\, dr$. Let $T\colon \mathbb{R}^2 \to \mathbb{R}$ denote an arbitrary statistic and

$$A(t) = \left\{(x_1, x_2) \in \mathbb{R}^2 \colon T(x_1, x_2) < t\right\}$$

a sublevel set generated by it. Then the value at the point t of the cdf of $T(X)$ is

$$F_{T,g,p}(t) = P\left(T(X) < t\right) = \Phi_{g,p}\left(A(t)\right).$$

Using (2.1), it follows

$$F_{T,g,p}(t) = \frac{1}{I_{2,g,p}} \int_0^\infty \frac{AL_{p,q}\left([r^{-1}A(t)] \cap S_{2,p}\right)}{AL_{p,q}\left(S_{2,p}\right)} rg(r^p)\, dr.$$

The constant $AL_{p,q}\left(S_{2,p}\right)$ in the last formula can also be interpreted geometrically. It complies with both the suitably defined non-Euclidean arc-length or circumference of the $l_{2,p}$-unit circle and two times the area content of $K_{2,p}$, i.e. with $2\pi(p)$, where the the $l_{2,p}$-circle number $\pi(p) = 2\left(\Gamma\left(\frac{1}{p}\right)\right)^2 / p\Gamma\left(\frac{2}{p}\right)$ is a generalization of the circle number π within the context of a non-Euclidian geometry, see Richter (2008a,b).

If we are given a concrete statistic $T = T(X)$, which is derived from a sample vector $X \sim \Phi_{g,p}$, the calculation of $AL_{p,q}\left([r^{-1}A(t)] \cap S_{2,p}\right)$ always yields an integral representation of the cdf $F_{T,p}(t)$.

Let $Pol_p\colon [0,\infty) \times [0, 2\pi) \to \mathbb{R}^2$ denote the p-generalized polar coordinate transformation defined in Richter (2007). Let further $\varphi \to Pol_p^\star(\varphi) = Pol_p(1, \varphi)$ be its restriction to $r = 1$ and $Pol_p^{\star -1}$ the corresponding inverse mapping. According to Richter (2008a,b, 2009), the p-generalized uniform distribution on $S_{2,p}$ may be represented as

$$\omega_p(M) = \frac{1}{2\pi(p)} \int_{Pol_p^{\star -1}(M)} \frac{d\varphi}{N_p^2(\varphi)}, \quad M \in \mathfrak{B}^2 \cap S_{2,p}$$

with $N_p(\varphi) = \left(|\cos\varphi|^p + |\sin\varphi|^p\right)^{\frac{1}{p}}$. Hence, an alternative representation of $\Phi_{g,p}$ is given by

$$\Phi_{g,p}\left(A(t)\right) = \frac{1}{2\pi(p) I_{2,g,p}} \int_0^\infty \int_{Pol_p^{\star -1}([r^{-1}A(t)] \cap S_{2,p})} \frac{d\varphi}{N_p^2(\varphi)}\, rg(r^p)\, dr.$$

In what follows, we assume that $Pol_p^{\star -1}\left([r^{-1}A(t)] \cap S_{2,p}\right)$ is an interval, say (γ, δ), where $\gamma = \gamma(A(t), r)$ and $\delta = \delta(A(t), r)$. Then, we shall make use of the notation $\mathfrak{G}_p(\gamma, \delta) = \mathfrak{F}_p(A(t), r)$, i.e.,

$$\mathfrak{G}_p(\gamma, \delta) = \frac{1}{2\pi(p)} \int_\gamma^\delta \frac{d\varphi}{N_p^2(\varphi)}.$$

Thus,

$$F_{T,g,p}(t) = \frac{1}{I_{2,g,p}} \int_0^\infty \mathfrak{G}_p(\gamma, \delta)\, rg(r^p)\, dr.$$

As a conclusion, it suffices to determine the ipf of the set $A(t)$ which is generated by the particular statistic T. To achieve this aim, the $l_{2,q}$-arc-length (p-generalized surface content) of the set $\frac{1}{r}A(t) \cap S_{2,p}$ has to be computed for each $t \in \mathbb{R}$ and $r > 0$, respectively, where $\frac{1}{p} + \frac{1}{q} = 1$. In order to do this, one can use the integral representation of the p-generalized uniform distribution on $S_{2,p}$ in combination with the image of the inverse mapping $Pol_p^{\star -1}\left(\frac{1}{r}A(t) \cap S_{2,p}\right)$. This strategy will be used in Sections 3, 4, and 5 to obtain the exact distributions of the extreme value, product, and ratio statistic. For some other examples, we refer to Günzel et al (2012), Kalke et al (2013), and the p-generalized χ^2-, t-, and F-distributions and their g-generalizations in Richter (2009).

3 Extreme values

The distributions of the extreme values of a finite number of independent and identically distributed random variables have already been studied in Gumbel (1958). For the corresponding case of increasing sample size see, e.g., David (1981). The exact distribution of the maximum of absolutely continuous dependent random variables was considered in Arellano-Valle and Genton (2008) and Jamalizadeh and Balakrishnan (2010).

In this section, we derive representations for the cdf and the pdf of the maximum statistic M, i.e. of $M(X) = \max\{X_1, X_2\}$, and the minimum statistic m, i.e. of $m(X) = \min\{X_1, X_2\}$, where $X = (X_1, X_2) \sim \Phi_{g,p}$ with arbitrary dgf g and parameter $p > 0$.

The sublevel sets generated by M are

$$A(t) = \left\{(x_1, x_2) \in \mathbb{R}^2 \colon \max\{x_1, x_2\} < t\right\}, \quad t \in \mathbb{R}$$

(see Figure 3.1). Obviously,

$$\begin{aligned}\frac{1}{r}A(t) &= \left\{\left(\frac{x_1}{r}, \frac{x_2}{r}\right) \in \mathbb{R}^2 \colon \max\{x_1, x_2\} < t\right\} \\ &= \left\{(x_1, x_2) \in \mathbb{R}^2 \colon \max\{x_1, x_2\} < \frac{t}{r}\right\}.\end{aligned}$$

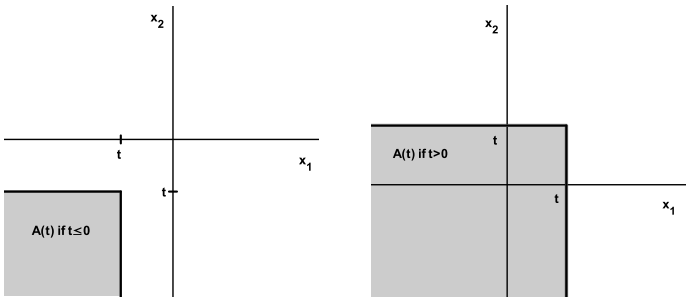

Fig. 3.1: The sublevel sets $A(t)$ in the case $T(X) = M(X)$, which are displayed for two particular $t \in \mathbb{R}$, are rectangular cones with vertices in $(t, t) \in \mathbb{R}^2$.

The intersections of the sets $\frac{1}{r}A(t)$ with the $l_{2,p}$-unit circle $S_{2,p}$, which are needed to determine the $l_{2,p}$-circle ipf of the set $A(t)$, are distinguished in five cases, see Figure 3.2, since there are substantial differences in the structur of intersections and, hence, in the structur of ipf if the variable t changes, respectively. It turns out that, for fixed t, the classification of these typical situations for r, $r > 0$, is one and the same for all parameters $p > 0$. The cases indicated by a) and e) in Figure 3.2 may be considered as the trivial cases for which the ipf of $A(t)$ is equal to zero or one, respectively.

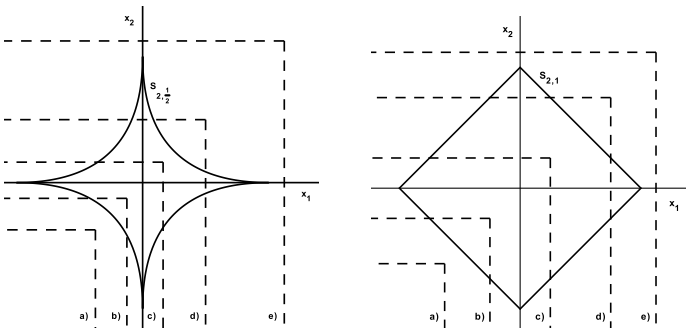

Fig. 3.2: The typically distinguished five cases *a*), *b*), *c*), *d*), and *e*), which correspond to typical regions of values of the variable t, are illustrated on the left for $p = \frac{1}{2}$ and on the right for $p = 1$, and are one and the same for all parameters $p > 0$.

Let us denote the cdf of $M(X)$ by $F_{M,g,p}$.

Theorem 1 *If $t \leq 0$, the cdf of $M(X)$ satisfies the representation*

$$F_{M,g,p}(t) = \frac{1}{I_{2,g,p}} \int_{-\sqrt[p]{2}t}^{\infty} \mathfrak{G}_p\left(\pi + \alpha, \frac{3\pi}{2} - \alpha\right) rg(r^p)\, dr,$$

and if $t > 0$,

$$F_{M,g,p}(t) = \frac{1}{I_{2,g,p}} \left[\int_0^t rg(r^p)\, dr + \int_t^{\sqrt[p]{2}t} \left[\mathfrak{G}_p\left(\pi - \alpha, \tfrac{3\pi}{2} + \alpha\right) + \mathfrak{G}_p\left(\tfrac{\pi}{2} - \alpha, \alpha\right)\right] rg(r^p)\, dr + \int_{\sqrt[p]{2}t}^{\infty} \mathfrak{G}_p\left(\pi - \alpha, \tfrac{3\pi}{2} + \alpha\right) rg(r^p)\, dr \right],$$

where $\alpha = \alpha(r,t) = \arctan\left(\dfrac{|t|}{\sqrt[p]{r^p - |t|^p}}\right)$.

Proof Let $t \leq 0$ and consider $A(t) \cap S_{2,p}(r)$, see Figure 3.3.

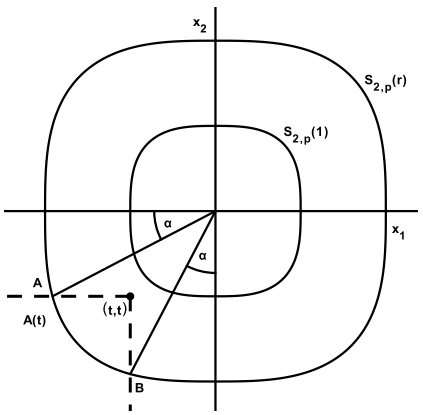

Fig. 3.3: The typical case b) in Figure 3.2 of the intersection of $A(t)$ and $S_{2,p}(r)$ is pictured in case of a particular $t \leq 0$ and $p = 3$.

This intersection is not empty if the p-functional of the point (t,t) is less than or equal to r, i.e.

$$r \geq |(t,t)|_p = (|t|^p + |t|^p)^{\frac{1}{p}} = -\sqrt[p]{2}t.$$

This inequality describes for which $r > 0$ we are dealing with a typical situation which is indicated by b) in Figure 3.2. Let A and B denote the intersection points of $S_{2,p}(r)$ and the boundary $\partial A(t)$ of $A(t)$. The rays starting in the origin and passing through the points A or B build angles of the

same magnitude α with the x- and y- coordinate axes, respectively. The point $A = (x,t) \in S_{2,p}(r)$ with $x \leq 0$ satisfies the equation $r^p = |(x,t)|_p^p$, hence $x = -\sqrt[p]{r^p - |t|^p}$. It follows

$$\tan(\alpha) = \frac{-t}{\sqrt[p]{r^p - |t|^p}} \quad \text{and} \quad \alpha = \alpha(r,t) = \arctan\left(\frac{-t}{\sqrt[p]{r^p - |t|^p}}\right).$$

Hence,

$$Pol_p^{*-1}\left(\left[r^{-1}A(t)\right] \cap S_{2,p}\right) = \left[\pi + \alpha, \frac{3\pi}{2} - \alpha\right],$$

and the value of the ipf of the set $A(t)$ at the point r is

$$\mathfrak{G}_p\left(\pi + \alpha, \frac{3\pi}{2} - \alpha\right) \quad \text{with} \quad \alpha = \arctan\left(\frac{-t}{\sqrt[p]{r^p - |t|^p}}\right).$$

Let now $t > 0$ and consider $A(t) \cap S_{2,p}(r)$ first for r according to the typical situation c) in Figure 3.2 and then according to situation d), see Figures 3.4a and 3.4b, respectively.

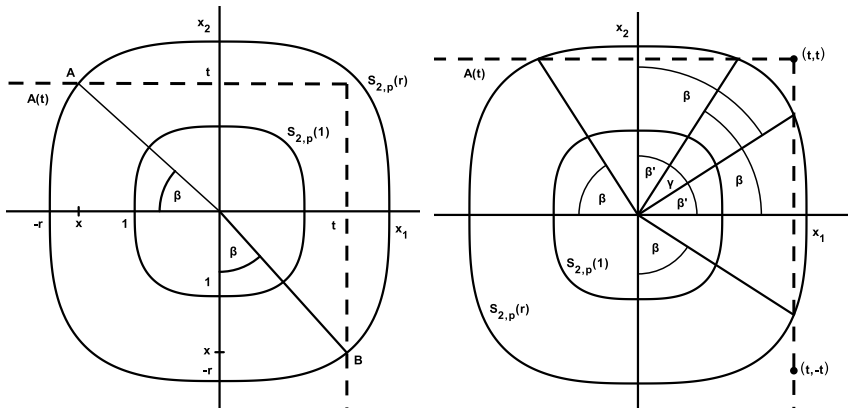

Fig. 3.4: The typical cases c) and d) in Figure 3.2 of the intersection of $A(t)$ and $S_{2,p}(r)$ are shown in case of particular $t > 0$ and $p = 3$.

In the case c) in Figure 3.2, the point (t,t) is inside of or on the p-circle with p-radius r, i.e. $r \geq |(t,t)|_p = \sqrt[p]{2}t$ or $r \in [\sqrt[p]{2}t, \infty)$. We denote the intersection points of $S_{2,p}(r)$ and $\partial A(t)$ by $A = (x,t)$ and $B = (t,x)$ with $x < 0$. The rays starting in the origin and passing through the points A or B build angles of the same magnitude β with the negative x- and the negative y-coordinate

axes, respectively. The points $A = (x, t)$ and $B = (t, x)$ with $x < 0$ satisfy the equation $r^p = |(x, t)|_p^p$, hence $x = -\sqrt[p]{r^p - t^p}$. It follows that

$$\tan(\beta) = \frac{|t|}{|x|} = \frac{t}{\sqrt[p]{r^p - |t|^p}} \quad \text{and} \quad \beta = \beta(r, t) = \arctan\left(\frac{t}{\sqrt[p]{r^p - |t|^p}}\right).$$

Consequently,

$$Pol_p^{*-1}\left(\left[r^{-1}A(t)\right] \cap S_{2,p}\right) = \left[\pi - \beta, \frac{3\pi}{2} + \beta\right],$$

and the value of the ipf of the set $A(t)$ at the point r is $\mathfrak{G}_p\left(\pi - \beta, \frac{3\pi}{2} + \beta\right)$.

Analogously, the case shown in Figure 3.4b and corresponding to the typical case d) in Figure 3.2 arises if $t \le r < |(t, t)|_p = \sqrt[p]{2}t$, i.e. $r \in [t, \sqrt[p]{2}t)$. The angle β is defined in the same way as in Figure 3.4a. The angle γ has the same magnitude as the length of the interval $\left[\beta', \frac{\pi}{2} - \beta'\right] = \left[\frac{\pi}{2} - \beta, \beta\right]$. Thus,

$$Pol_p^{*-1}\left(\left[r^{-1}A(t)\right] \cap S_{2,p}\right) = \left[\pi - \beta, \frac{3\pi}{2} + \beta\right] \cup \left[\frac{\pi}{2} - \beta, \beta\right],$$

and the ipf is

$$\mathfrak{G}_p\left(\pi - \beta, \frac{3\pi}{2} + \beta\right) + \mathfrak{G}_p\left(\frac{\pi}{2} - \beta, \beta\right).$$

In the last case, which corresponds to the typical case e) in Figure 3.2, the p-circle with p-radius r belongs completely to the set $A(t)$. Thus, the ipf equals 1. Finally, notice that $\alpha(r, t) = \beta(r, t)$. □

Figure 3.5 shows the cdf $F_{M,g_p,p}$ for different values of p, according to Theorem 1.

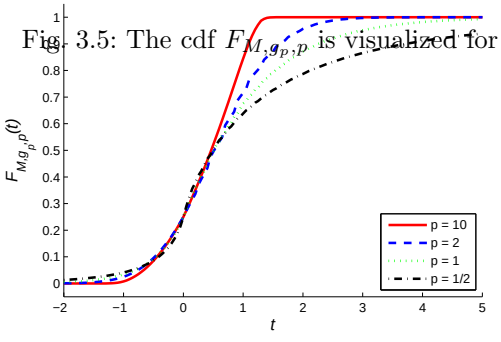

Fig. 3.5: The cdf $F_{M,g_p,p}$ is visualized for several values of p.

Corollary 1 *If $t<0$, then the pdf $f_{M,g,p}$ of $M(X)$ is*

$$f_{M,g,p}(t)=\frac{1}{2\pi(p)I_{2,g,p}}\int\limits_{-\sqrt[p]{2}t}^{\infty} rg(r^p)\beta\left(N_p^{-2}\left(\tfrac{3\pi}{2}-\alpha\right)+N_p^{-2}\left(\pi+\alpha\right)\right)\,dr,$$

and if $t>0$, then

$$f_{M,g,p}(t)=\frac{1}{2\pi(p)I_{2,g,p}}\left[\int\limits_{t}^{\infty} rg(r^p)\beta\left(N_p^{-2}\left(\tfrac{3\pi}{2}+\alpha\right)+N_p^{-2}\left(\pi-\alpha\right)\right)\,dr + \int\limits_{t}^{\sqrt[p]{2}t} rg(r^p)\beta\left(N_p^{-2}\left(\alpha\right)+N_p^{-2}\left(\tfrac{\pi}{2}-\alpha\right)\right)\,dr\right]$$

where $\alpha=\alpha\left(r,t\right)=\arctan\left(\frac{|t|}{\sqrt[p]{r^p-|t|^p}}\right)$ and

$$\beta=\beta\left(r,t\right)=\frac{\left(r^p-|t|^p\right)^{\frac{1}{p}}+|t|^p\cdot\left(r^p-|t|^p\right)^{-\frac{p-1}{p}}}{\left(r^p-|t|^p\right)^{\frac{2}{p}}+t^2}.$$

Proof Let $t<0$ and put

$$P\left(r,t\right)=rg(r^p)\mathfrak{G}_p\left(\pi+\alpha,\frac{3\pi}{2}-\alpha\right)=\frac{1}{2\pi(p)}rg(r^p)\int\limits_{\pi+\alpha}^{\frac{3\pi}{2}-\alpha}\frac{d\varphi}{N_p^2\left(\varphi\right)}.$$

Making use of the Leibniz integral rule, it follows for $f_{M,g,p}(t)=F'_{M,g,p}(t)$ that

$$f_{M,g,p}(t)=\frac{1}{2\pi(p)I_{2,g,p}}\left[\int\limits_{-\sqrt[p]{2}t}^{\infty}\frac{\partial}{\partial t}P\left(r,t\right)\,dr-\left(-\sqrt[p]{2}\right)\cdot P\left(-\sqrt[p]{2}t,t\right)\right]$$

where, because of $\alpha\left(-\sqrt[p]{2}t,t\right)=\frac{\pi}{4}$,

$$P\left(-\sqrt[p]{2}t,t\right)=\frac{1}{2\pi(p)}\left(-\sqrt[p]{2}t\right)\cdot g\left(2(-t)^p\right)\cdot\int\limits_{\frac{5}{4}\pi}^{\frac{5}{4}\pi}\frac{d\varphi}{N_p^2\left(\varphi\right)}=0.$$

Using the Leibniz integral rule again, we get

$$\frac{\partial}{\partial t}P\left(r,t\right)=\frac{1}{2\pi(p)}rg(r^p)\beta\left(N_p^{-2}\left(\frac{3\pi}{2}-\alpha\right)+N_p^{-2}\left(\pi+\alpha\right)\right),$$

where $\beta=\beta\left(r,t\right)=-\frac{\partial}{\partial t}\alpha\left(r,t\right)$ is the partial derivative of α w.r.t. t. This proves the first part of Corollary 1. The second part $t>0$ follows by analogous considerations. □

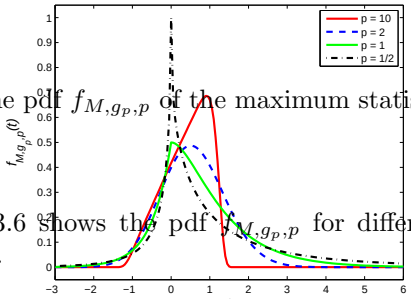

Fig. 3.6: The pdf $f_{M,g_p,p}$ of the maximum statistic is shown for several values of p.

Figure 3.6 shows the pdf $f_{M,g_p,p}$ for different values of p, according to Corollary 1.

Remark 1 In an analogous way as in the proof of Theorem 1, the cdf of $M(X)$ can be determined specifically for the cases of $p \in \{1,2\}$. This way, one gets

$$F_{M,g,1}(t) = \frac{1}{I_{2,g,1}} \begin{cases} \int\limits_{-2t}^{\infty} \left(\frac{r}{4} + \frac{t}{2}\right) g(r)\, dr & , \ t \le 0 \\ \frac{1}{4} I_{2,g,1} + \frac{3}{4} \int\limits_{0}^{t} r g(r)\, dr & \\ \quad + \frac{1}{4} \int\limits_{t}^{2t} (4t - r)\, g(r)\, dr + \frac{1}{2} \int\limits_{2t}^{\infty} t g(r)\, dr & , \ t > 0 \end{cases}$$

and

$$F_{M,g,2}(t) = \frac{1}{I_{2,g,2}} \begin{cases} \int\limits_{-\sqrt{2}t}^{\infty} \left(\frac{1}{4} + \frac{\alpha}{\pi}\right) r g(r^2)\, dr & , \ t \le 0 \\ \frac{1}{4} I_{2,g,2} + \frac{3}{4} \int\limits_{0}^{t} r g(r^2)\, dr & \\ \quad + \frac{1}{2\pi} \int\limits_{t}^{\sqrt{2}t} \left(4\beta - \frac{\pi}{2}\right) r g(r^2)\, dr & , \ t > 0 \\ \quad + \frac{1}{\pi} \int\limits_{\sqrt{2}t}^{\infty} \beta r g(r^2)\, dr & \end{cases}$$

with $\alpha = \alpha(r,t) = \arcsin\left(\frac{|t|}{r}\right)$ while, on the other hand, one gets slightly different formulae by just specializing the result of Theorem 1 for $p = 1$ and $p = 2$, respectively. Using suitable trigonometric identities, it can be shown, however, that after some transformations these representations coincide with those given above.

Let $F_{m,g,p}$ and $f_{m,g,p}$ denote the cdf and the pdf of the minimum statistic $m(X)$, i.e. $m(X) = \min\{X_1, X_2\}$, where $X = (X_1, X_2) \sim \Phi_{g,p}$ with arbitrary dgf g and parameter $p > 0$.

Corollary 2 *The cdf $F_{m,g,p}$ and the pdf $f_{m,g,p}$ of $m(X)$ satisfy the representations $F_{m,g,p}(t) = 1 - F_{M,g,p}(-t)$ and $f_{m,g,p}(t) = f_{M,g,p}(-t)$ for all $t \in \mathbb{R}$.*

Proof By using the $l_{2,p}$-symmetry of the distribution of X and continuity of X, one gets

$$\begin{aligned} F_{m,g,p}(t) &= 1 - P(\min\{X_1, X_2\} \geq t) \\ &= 1 - P(\max\{X_1, X_2\} \leq -t) = 1 - F_{M,g,p}(-t). \end{aligned}$$

The second statement follows by taking the derivative of $F_{m,g,p}$ with the help of the chain rule. □

In particular, the pdf of $m(X)$ is the mirror image of the pdf of $M(X)$ in the mirror line $t = 0$, see Figure 3.7 and cf. Figure 3.6. Hence, the cdf $F_{m,g,p}$ of $m(X)$ is the point reflection of the cdf $F_{M,g,p}$ of $M(X)$ w.r.t. the point $\left(0, \frac{1}{2}\right)$.

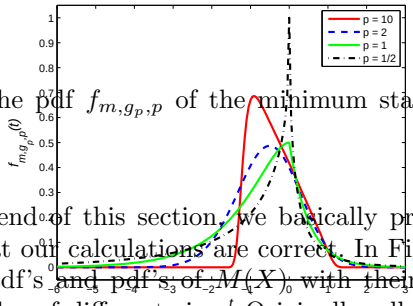

Fig. 3.7: The pdf $f_{m,g_p,p}$ of the minimum statistic is illustrated for several values of p.

At the end of this section, we basically present a numerical demonstration for that our calculations are correct. In Figures 3.8 and 3.9, we compare the exact cdf's and pdf's of $M(X)$ with their simulations which are based upon samples of different sizes. Originally, all simulations were done for the power-exponential distribution with different values of the parameter p, $p > 0$, using the R-module 'pgnorm' which has arisen from Kalke and Richter (2013). However, on this very elementary level of visual inspection, there were no remarkable differences between all figures made for different values of p, $p > 0$. That is why we restrict our visualization of effects of the simulation sample size n here to the Gaussian case.

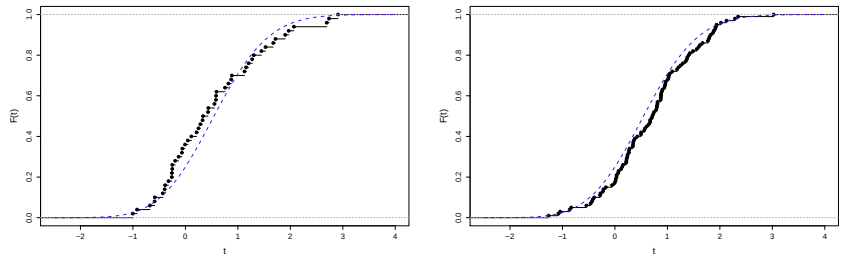

(a) $n = 50$ (b) $n = 100$

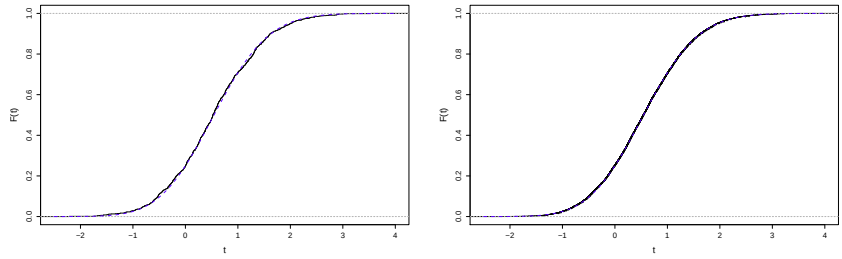

(c) $n = 10^3$ (d) $n = 10^4$

Fig. 3.8: For increasing sample sizes n, the simulated cdf $F(t) = \widehat{F}_{M,g_2,2}(t)$ of the maximum statistic $M(X)$ from a Gaussian sample approaches the exact cdf which is shown by a dashed line.

It may be a very rough first conclusion from these particular simulation results in the integral and the local cases, i.e. for the cdf and the pdf, to formulate the impressions that quite large sample sizes are needed for approximating an exact distribution or density by simulation and, in particular, that local comparison studies of the present type need in some sense a ten times bigger sample size than integral ones.

4 Products

In this section, we derive representations of the cdf and the pdf of the product statistic $P(X) = X_1 \cdot X_2$, where $X = (X_1, X_2) \sim \Phi_{g,p}$ with arbitrary dgf g and parameter $p > 0$. The special cases $p = 1$ and $p = 2$ were considered in Kalke et al (2013) and some of the references cited therein. The statistic P generates the sublevel sets

$$A(t) = \left\{(x_1, x_2) \in \mathbb{R}^2 : x_1 x_2 < t\right\}, \quad t \in \mathbb{R},$$

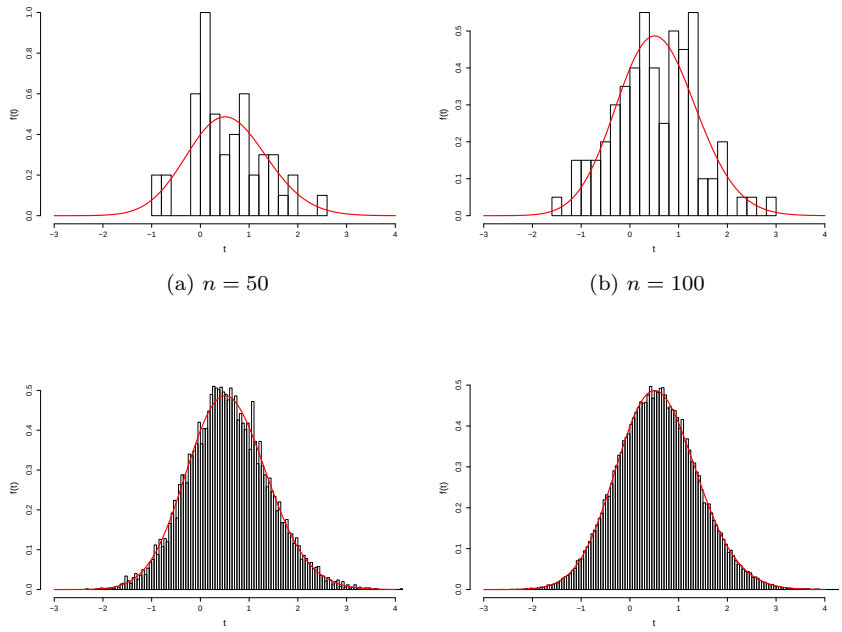

(a) $n = 50$ (b) $n = 100$

(c) $n = 10^4$ (d) $n = 10^5$

Fig. 3.9: The simulated pdf $f(t) = \widehat{f}_{M,g_2,2}(t)$ of $M(X)$ in case of a Gaussian sample, displayed by a histogram plot of relative frequencies, approaches the exact pdf for inceasing sample sizes n.

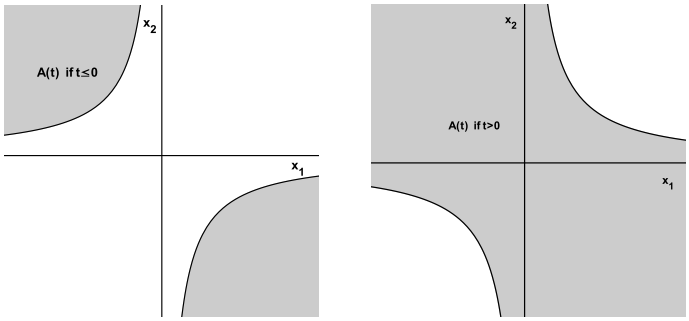

Fig. 4.1: The sublevel set $A(t)$ generated by the product statistic is shown for a negative value of t (on the left side) and a positive value of t (on the right side).

see Figure 4.1. Let us denote the cdf of $P(X)$ by $F_{P,g,p}$.

Theorem 2 *The cdf of $P(X)$ satisfies the representation*

$$F_{P,g,p}(t) = \begin{cases} \frac{2}{I_{2,g,p}} \int\limits_{\sqrt[p]{2}\sqrt{|t|}}^{\infty} \mathfrak{G}_p\left(\pi-\alpha, \frac{\pi}{2}+\alpha\right) rg(r^p)\, dr & \text{if } t \le 0 \\ 1 - \frac{2}{I_{2,g,p}} \int\limits_{\sqrt[p]{2}\sqrt{t}}^{\infty} \mathfrak{G}_p\left(\pi-\alpha, \frac{\pi}{2}+\alpha\right) rg(r^p)\, dr & \text{if } t > 0 \end{cases},$$

where

$$\alpha = \alpha(r,t) = \arccos\left(\frac{\sqrt[p]{\frac{1}{2} - \sqrt{\frac{1}{4} - \left(\frac{|t|}{r^2}\right)^p}}}{\left| \left(\sqrt[p]{\frac{1}{2} - \sqrt{\frac{1}{4} - \left(\frac{|t|}{r^2}\right)^p}}, \sqrt[p]{\frac{1}{2} + \sqrt{\frac{1}{4} - \left(\frac{|t|}{r^2}\right)^p}} \right) \right|_2} \right).$$

Proof Consider the intersection $\frac{1}{r}A(t) \cap S_{2,p}$. Let $P = (x_{1_1}, x_{2_2})$ and $Q = (x_{1_2}, x_{2_1})$ denote the intersection points of $S_{2,p}$ and the boundary $\partial\left(\frac{1}{r}A(t)\right)$ of $\frac{1}{r}A(t)$, see Figure 4.2.

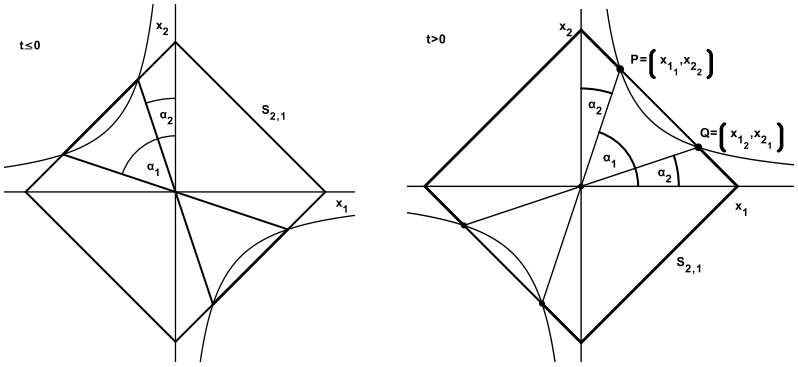

Fig. 4.2: The intersections of $\frac{1}{r}A(t)$ and $S_{2,p}$ are displayed for $p = 1$, a specific $r > 0$ and a particular $t \le 0$ (left side) as well as a particular $t > 0$ (right side).

The solutions of the corresponding equation system $x_1 x_2 = \frac{t}{r^2}$ and $|x_1|^p + |x_2|^p = 1$ are for $i = 1, 2$

$$x_{i_1} = \sqrt[p]{\frac{1}{2} - \sqrt{\frac{1}{4} - \left(\frac{|t|}{r^2}\right)^p}} \quad \text{and} \quad x_{i_2} = \sqrt[p]{\frac{1}{2} + \sqrt{\frac{1}{4} - \left(\frac{|t|}{r^2}\right)^p}}.$$

Furthermore, $\frac{1}{r}A(t) \cap S_{2,p}$ is the empty set if $r \leq \sqrt[p]{2}\sqrt{|t|}$. The angles α_1 and α_2, see Figure 4.2, satisfy the equations

$$\alpha_1 = \arccos\left(\frac{x_{i_1}}{d}\right) \quad \text{and} \quad \alpha_2 = \arccos\left(\frac{x_{i_2}}{s}\right),$$

where $d = |(x_{1_1}, x_{2_2})|_2 = |(x_{1_2}, x_{2_1})|_2 = s$, and $\alpha_1 + \alpha_2 = \frac{\pi}{2}$. As $\frac{1}{r}A(t) \cap S_{2,p}$ in the case $t \leq 0$ is the reflection on the ordinate axis of $\frac{1}{r}A(t) \cap S_{2,p}$ from the case $t > 0$, the angles of interest have the same magnitudes in both cases. Analogously to the proof of Theorem 1,

$$Pol_p^{*-1}\left(\left[r^{-1}A(t)\right] \cap S_{2,p}\right) = [\pi - \alpha_1, \frac{\pi}{2} + \alpha_1] \cup [2\pi - \alpha_1, \frac{3\pi}{2} + \alpha_1]$$

if $t \leq 0$ and

$$Pol_p^{*-1}\left(\left[r^{-1}A(t)\right] \cap S_{2,p}\right) = [0, 2\pi] \setminus ([\alpha_2, \alpha_1] \cup [\pi + \alpha_2, \pi + \alpha_1])$$

if $t > 0$. Hence, if $t \leq 0$, the ipf is

$$\mathfrak{F}_p\left(A(t), r\right) = \mathfrak{G}_p\left(\pi - \alpha_1, \frac{\pi}{2} + \alpha_1\right) + \mathfrak{G}_p\left(2\pi - \alpha_1, \frac{3\pi}{2} + \alpha_1\right)$$

which coincides for symmetry reasons with

$$2\mathfrak{G}_p\left(\pi - \alpha_1, \frac{\pi}{2} + \alpha_1\right) = \frac{1}{\pi(p)} \int_{\pi - \alpha_1}^{\frac{\pi}{2} + \alpha_1} \frac{d\varphi}{N_p^2(\varphi)}.$$

If $t > 0$,

$$\begin{aligned}\mathfrak{F}_p(A(t), r) &= 1 - \frac{1}{\pi(p)} \int_{\alpha_2}^{\alpha_1} \frac{d\varphi}{N_p^2(\varphi)} = 1 - 2\mathfrak{G}_p\left(\alpha_2, \alpha_1\right) \\ &= 1 - 2\mathfrak{G}_p\left(\frac{\pi}{2} - \alpha_1, \alpha_1\right) = 1 - 2\mathfrak{G}_p\left(\pi - \alpha_1, \frac{\pi}{2} + \alpha_1\right),\end{aligned}$$

since $N_p^{-2}\left(\frac{\pi}{2} + \varphi\right) = N_p^{-2}\left(\varphi\right)$. □

Figure 4.3 shows the cdf $F_{P,g_p,p}$ for different values of p.

Corollary 3 *The value of the pdf $f_{P,g,p}$ of $P(X)$ at the point $t \in \mathbb{R} \setminus \{0\}$ is*

$$f_{P,g,p}(t) = \frac{1}{I_{2,g,p} \cdot \pi(p)} \int_{\sqrt[p]{2}\sqrt{|t|}}^{\infty} rg(r^p)\beta\left(N_p^{-2}\left(\frac{\pi}{2} + \alpha\right) + N_p^{-2}\left(\pi - \alpha\right)\right) dr,$$

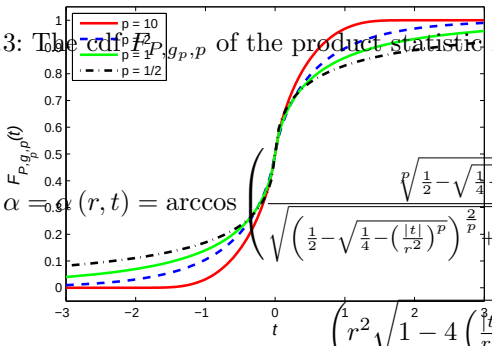

Fig. 4.3: The cdf $F_{P,g_p,p}$ of the product statistic is shown for several values of p.

where $\alpha = \alpha(r,t) = \arccos\left(\frac{\sqrt[p]{\frac{1}{2}-\sqrt{\frac{1}{4}-\left(\frac{|t|}{r^2}\right)^p}}}{\sqrt{\left(\frac{1}{2}-\sqrt{\frac{1}{4}-\left(\frac{|t|}{r^2}\right)^p}\right)^{\frac{2}{p}}+\left(\frac{1}{2}+\sqrt{\frac{1}{4}-\left(\frac{|t|}{r^2}\right)^p}\right)^{\frac{2}{p}}}}\right)$, *and*

$$\beta = \beta(r,t) = \frac{\left(r^2\sqrt{1-4\left(\frac{|t|}{r^2}\right)^p}\right)^{-1}}{\left(\left(\frac{1}{2}-\frac{1}{2}\sqrt{1-4\left(\frac{|t|}{r^2}\right)^p}\right)^{\frac{2}{p}}+\left(\frac{1}{2}+\frac{1}{2}\sqrt{1-4\left(\frac{|t|}{r^2}\right)^p}\right)^{\frac{2}{p}}\right)}.$$

Proof Let $t<0$ and put

$$P(r,t) = rg(r^p)\int\limits_{\pi-\alpha}^{\frac{\pi}{2}+\alpha}\frac{d\varphi}{N_p^2(\varphi)}.$$

Using the Leibniz integral rule, it follows

$$f_{P,g,p}(t) = \frac{1}{I_{2,g,p}\cdot\pi(p)}\left[\int\limits_{\sqrt[p]{2}\sqrt{-t}}^{\infty}\frac{d}{dt}P(r,t)\,dr - \left(\frac{-\sqrt[p]{2}}{2\sqrt{-t}}\right)P\left(\sqrt[p]{2}\sqrt{-t},t\right)\right].$$

With $\alpha\left(\sqrt[p]{2}\sqrt{-t},t\right)=\frac{\pi}{4}$, we have

$$P\left(\sqrt[p]{2}\sqrt{-t},t\right) = \sqrt[p]{2}\sqrt{-t}\,g\left(2(-t)^{\frac{p}{2}}\right)\int\limits_{\frac{3\pi}{4}}^{\frac{3\pi}{4}}\frac{d\varphi}{N_p^2(\varphi)} = 0.$$

Making use of the Leibniz integral rule again, we receive

$$\frac{\partial}{\partial t}P\left(r,t\right)=rg(r^p)\beta\left(N_p^{-2}\left(\frac{\pi}{2}+\alpha\right)+N_p^{-2}\left(\pi-\alpha\right)\right)\ ,$$

where $\beta=\beta\left(r,t\right)=\frac{\partial}{\partial t}\alpha\left(r,t\right)$ is the partial derivative of α w.r.t. t. This proves the first part of Corollary 3. In an analogous manner, case $t>0$ has been considered. □

Figure 4.4 shows the pdf $f_{P,g_p,p}$ for several values of p.

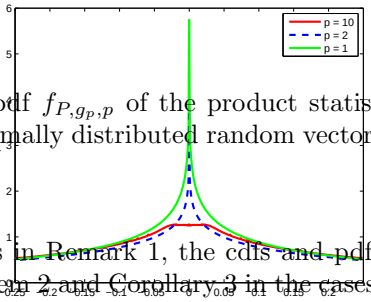

Fig. 4.4: The pdf $f_{P,g_p,p}$ of the product statistic P of a two-dimensional p-generalized normally distributed random vector is plotted for several values of p.

Similarly as in Remark 1, the cdfs and pdfs of $P(X)$ resulting from specializing Theorem 2 and Corollary 3 in the cases $p=1$ and $p=2$ can be transformed into the corresponding representations given in Kalke et al (2013) by using some trigonometric identities. Analogous statements hold for the cdf and the pdf of the ratio statistic $R(X)$ and are given in Theorem 3 and Corollary 4 below.

For the same reasons as at the end of Section 3, we restrict our visualization to the Gaussian case. Furthermore, only the sample sizes $n=100$ in case of cdf and $n=10^3$ in case of pdf will be considered (see Figures 4.5a and 4.5b), since all the figures for other sample sizes n reflect similar effects as at the end of Section 3. For corresponding illustrations for the ratio, see Figures 5.5a and 5.5b.

5 Ratios

In this section, we derive representations of the cdf and the pdf of the ratio statistic R, i.e. of $R(X)=\frac{X_1}{X_2}$, where $X=(X_1,X_2)\sim\Phi_{g,p}$ with arbitrary dgf g and parameter $p>0$. The special cases $p=1$ and $p=2$ were considered in

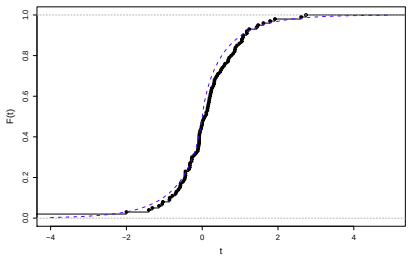

(a) The simulated cdf $F(t) = \widehat{F}_{P,g_2,2}(t)$ of $P(X)$ and exact cdf of $P(X)$ for a Gaussian sample of size $n = 10^2$ are displayed and reflect the correctness of our results numerically.

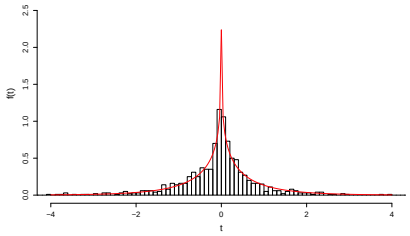

(b) The simulated pdf $f(t) = \widehat{f}_{P,g_2,2}(t)$ of $P(X)$ for a Gaussian sample of size $n = 10^3$ is close to the exact one.

Fig. 4.5

Kalke et al (2013) and some of the references cited therein. Further, it is shown in Szablowski (1998) that ratios of $l_{2,p}$-symmetric random variables follow a p-generalized Cauchy distribution. We consider the sublevel sets

$$A(t) = \left\{(x_1, x_2) \in \mathbb{R}^2 \colon \frac{x_1}{x_2} < t\right\}, \quad t \in \mathbb{R},$$

which are generated by the statistic R, see Figure 5.1.

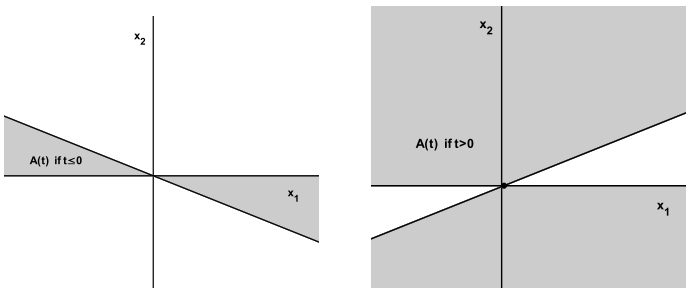

Fig. 5.1: In the case of the ratio, if $t \leq 0$, the sublevel set $A(t)$ and, if $t > 0$, its complement are double cones with vertex in the origin.

Let us denote the cdf of $R(X)$ by $F_{R,p}$.

Theorem 3 *The cdf of $R(X)$ satisfies the representation*

$$F_{R,p}(t) = \frac{1}{\pi(p)} \int\limits_{\frac{\pi}{2} - \arctan t}^{\pi} \frac{d\varphi}{N_p^2(\varphi)} = 2\mathfrak{G}_p\left(\frac{\pi}{2} - \arctan t, \pi\right), \quad t \in \mathbb{R}.$$

Proof Because of $A(t) = \frac{1}{r}A(t)$, $r > 0$, $A(t)$ is a double cone with vertex in the origin. Hence, the quantity

$$AL_{p,q}\left(r^{-1}\left[A(t) \cap S_{2,p}(r)\right]\right)$$

does not depend on the radius variable r. Therefore,

$$F_{R,p}(t) = \Phi_{g,p}(A(t)) = \mathfrak{F}_p(A(t), 1).$$

In particular, the cdf is independent of the dgf g.

We consider $A(t) \cap S_{2,p}$, see Figure 5.2. Since the set $A(t) \cap S_{2,p}$ is centrally symmetric w.r.t. the origin, in both cases $t \leq 0$ and $t > 0$ it is enough to determine one of the two intersection points of the line $x_2 = \frac{x_1}{t}$ with the $l_{2,p}$-unit circle $S_{2,p}$:

$$P_1 = \left(\frac{t}{(1+|t|^p)^{1/p}}, \frac{1}{(1+|t|^p)^{1/p}}\right) \quad \text{and} \quad P_2 = \left(\frac{-t}{(1+|t|^p)^{1/p}}, \frac{1}{(1+|t|^p)^{1/p}}\right).$$

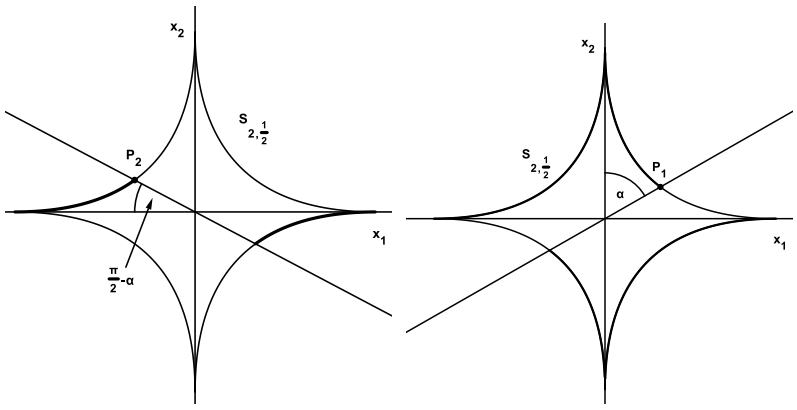

(a) $t \leq 0$ (b) $t > 0$

Fig. 5.2: The intersection of $A(t)$ and $S_{2,p}$ is visualized for $p = \frac{1}{2}$ and a particular $t \leq 0$ as well as a particular $t > 0$.

The ray starting in the origin and passing through the point P_1 builds an angle of the magnitude α with the x_2-coordinate axis. The magnitude of the angle, which is built by the ray starting in the origin and passing through the point P_2 with the negative x_1-coordinate axis, is $\frac{\pi}{2} - \alpha$ and it holds $\alpha = \arctan(|t|)$. Analogously to the proof of Theorem 1, it follows

$$Pol_p^{*-1}\left(A(t) \cap S_{2,p}\right) = \begin{cases} \left[\frac{\pi}{2} + \alpha, \pi\right] \cup \left[\frac{3\pi}{2} + \alpha, 2\pi\right] & , \text{ if } t \leq 0 \\ \left[\frac{\pi}{2} - \alpha, \pi\right] \cup \left[\frac{3\pi}{2} - \alpha, 2\pi\right] & , \text{ if } t > 0 \end{cases}.$$

From $\arctan(-t) = -\arctan(t)$ it follows

$$Pol_p^{\star -1}\left(A(t) \cap S_{2,p}\right) = \left[\frac{\pi}{2} - \arctan t, \pi\right] \cup \left[\frac{3\pi}{2} - \arctan t, 2\pi\right].$$

Hence,

$$\begin{aligned} F_{R,p}(t) &= \frac{1}{2\pi(p)} \left(\int\limits_{\frac{\pi}{2} - \arctan t}^{\pi} \frac{d\varphi}{N_p^2(\varphi)} + \int\limits_{\frac{3\pi}{2} - \arctan t}^{2\pi} \frac{d\varphi}{N_p^2(\varphi)} \right) \\ &= \mathfrak{G}_p\left(\frac{\pi}{2} - \arctan t, \pi\right) + \mathfrak{G}_p\left(\frac{3\pi}{2} - \arctan t, 2\pi\right). \end{aligned}$$

Because of the π-periodicity of the absolute values of the trigonometric functions, the function N_p is also π-periodic. □

Corollary 4 *The pdf $f_{R,p}$ of $R(X)$ is*

$$f_{R,p}(t) = \frac{1}{\pi(p)}(1 + |t|^p)^{-2/p} \quad , t \in \mathbb{R},$$

i.e. $R(X)$ is p-generalized Cauchy distributed.

Proof It follows from Theorem 3 that

$$\begin{aligned} f_{R,p}(t) &= \frac{1}{\pi(p)}(-1)(N_p^2\left(\tfrac{\pi}{2} - \arctan(t)\right))^{-1}(-1)\ \frac{1}{1+t^2} \\ &= \frac{1}{\pi(p)} \left(\left| \frac{1}{\sqrt{1+t^2}} \right|^p + \left(\frac{|t|}{\sqrt{1+t^2}} \right)^p \right)^{-2/p} \frac{1}{1+t^2} \\ &= \frac{1}{\pi(p)}(1 + |t|^p)^{-2/p}. \end{aligned}$$

□

Figures 5.3 and 5.4 show the cdf $F_{R,p}$ and the pdf $f_{R,p}$ for different values of p, respectively.

6 Application to failure rates

In this section, we deal with failure rates of the extreme value statistics. The IFR property was generally studied in Glaser (1980) and for the special cases of the minimum and maximum statistics of a multivariate normal distribution e.g. in Gupta and Gupta (2001). For the case $p = 1$, this result was proved recently in Nekoukhou and Alamatsaz (2012). In Batún-Cutz et al (2013), it was asked whether or not the IFR property of the extreme value statistics may also be verified in the case of a general $l_{2,p}$-symmetric vector distribution. Here, we are going to answer this question to a certain extent.

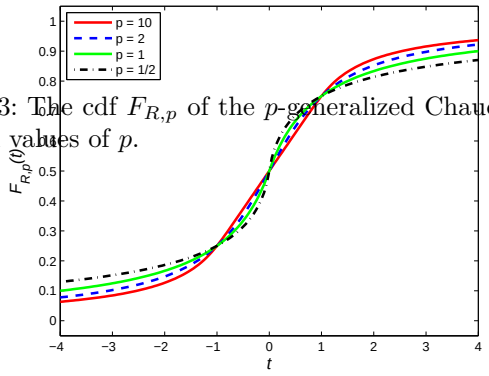

Fig. 5.3: The cdf $F_{R,p}$ of the p-generalized Chauchy distribution is shown for several values of p.

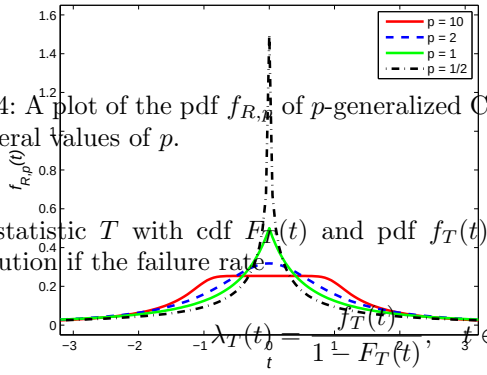

Fig. 5.4: A plot of the pdf $f_{R,p}$ of p-generalized Chauchy distribution is shown for several values of p.

A statistic T with cdf $F_T(t)$ and pdf $f_T(t)$ is said to possess an IFR-distribution if the failure rate

$$\lambda_T(t) = \frac{f_T(t)}{1 - F_T(t)}, \quad t \in \mathbb{R},$$

is a monotonically increasing function. Equivalently, the cdf $F_T(t)$ has IFR iff $\ln(1 - F_T(t))$ is a concave function. Because of

$$\frac{d^2}{dt^2} \ln(1 - F_T(t)) = -\frac{f_T'(t)(1 - F_T(t)) + (f_T(t))^2}{(1 - F_T(t))^2},$$

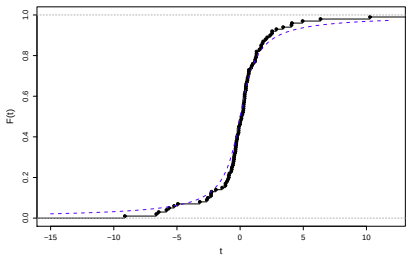

(a) The illustrations of the simulated cdf $F(t) = \widehat{F}_{R,g_2,2}(t)$ of $R(X)$ and exact cdf of $R(X)$ for a Gaussian sample of size $n = 10^2$ verify the accuracy of our results numerically.

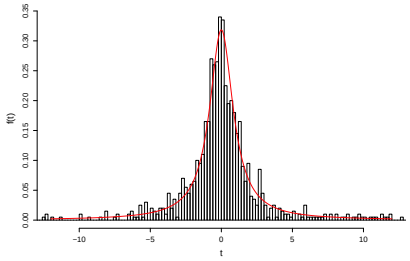

(b) Simulated pdf of the p-generalized Cauchy distribution is calculated after a simulation of the pdf $f(t) = \widehat{f}_{R,g_2,2}(t)$ of $R(X)$ for a Gaussian sample of size $n = 10^3$, and compared with the exact pdf of a p-generalized Cauchy random variable.

Fig. 5.5

$F_T(t)$ has IFR iff for all $t \in \mathbb{R}$

$$f'_T(t)\,(1 - F_T(t)) + (f_T(t))^2 \geq 0. \tag{6.1}$$

Theorem 4 *If $p \geq 1$, then the maximum statistic $M(X)$ of a bivariate p-power exponentially distributed random vector X satisfies the IFR-property.*

Proof According to Batún-Cutz et al (2013), the pdf of $M(X)$ given in Corollary 1 can be transformed into the representation

$$f_{M,g_p,p}(t) = 2\phi_p(t)\Phi_p(t), \quad t \in \mathbb{R},$$

where $\phi_p(t) = C_p e^{-\frac{|t|^p}{p}}$ is the pdf and $\Phi_p(t) = \int_{-\infty}^{t} \phi_p(s)\,ds$ is the cdf of a p-power exponential distribution and $C_p = \frac{p^{1-\frac{1}{p}}}{2\Gamma\left(\frac{1}{p}\right)}$ is the corresponding normalizing constant. If $t < 0$, then

$$f'_{M,g_p,p}(t) = 2\phi_p(t)[\Phi_p(t) \cdot (-t)^{p-1} + \phi_p(t)] \geq 0,$$

for arbitrary $p > 0$. Hence, (6.1) is fulfilled. From now on, let $t > 0$. Then,

$$f'_{M,g_p,p}(t) = 2\phi_p(t)[\phi_p(t) - t^{p-1}\Phi_p(t)]$$

and, therefore, (6.1) is satisfied iff $I_1(t) \geq 0$ where

$$I_1(t) = t^{p-1}\Phi_p(t)[\Phi_p^2(t) - 1] + \phi_p(t)[1 + \Phi_p^2(t)].$$

Note that

$$\lim_{t\to 0+} I_1(t) = \frac{5}{4}C_p = \frac{5p^{\frac{p-1}{p}}}{8\Gamma\left(\frac{1}{p}\right)}$$

iff $p \geq 1$. Hence, $\lim_{t\to 0+} I_1(t) > 0$ if $p \geq 1$. It remains to prove that there is no $t > 0$ such that $I_1(t) = 0$. Put

$$J_{lS}(t) = \frac{\phi_p(t)}{t^{p-1}} \quad \text{and} \quad J_{rS}(t) = \frac{\Phi_p(t)[1-\Phi_p^2(t)]}{1+\Phi_p^2(t)}.$$

Now we have to show that $J_{lS}(t) \neq J_{rS}(t)$ for all $t > 0$. By partial integration,

$$1 - \Phi_p(t) = J_{lS}(t) + C_p(1-p)\int_t^\infty z^{-p} e^{-\frac{z^p}{p}}\, dz,$$

hence,

$$\begin{aligned} J_{rS}(t) - J_{lS}(t) &= (1-\Phi_p(t))\left(1 - \frac{1-\Phi_p(t)}{1+\Phi_p^2(t)}\right) - J_{lS}(t) \\ &< (1-\Phi_p(t)) - J_{lS}(t) = C_p(1-p)\int_t^\infty z^{-p} e^{-\frac{z^p}{p}}\, dz \leq 0 \end{aligned}$$

if $p \geq 1$. Therefore, it follows

$$f'_{M,g_p,p}(t)\left(1 - F_{M,g_p,p}(t)\right) + \left(f_{M,g_p,p}(t)\right)^2 > 0$$

for all $t \in (0,\infty)$ and $p \geq 1$ and the IFR-property is proven if $p \geq 1$. □

In case of $p \in (0,1)$, we just refer to Figure 6.1 and point out that, in general, the maximum statistic has neither a monotonically increasing nor a monotonically decreasing failure rate for all positive arguments.

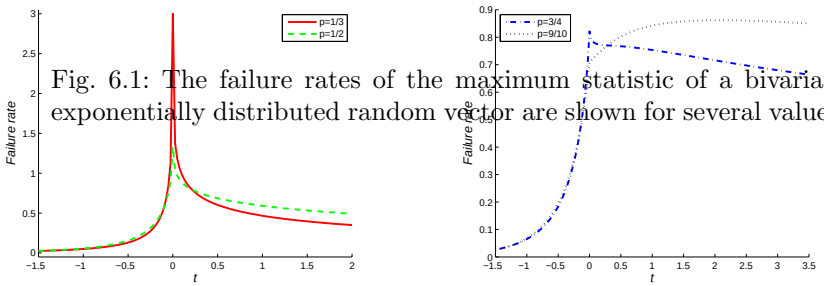

Fig. 6.1: The failure rates of the maximum statistic of a bivariate p-power exponentially distributed random vector are shown for several values of p. (M)

Corollary 5 *If $p \geq 1$, then the minimum statistic $m(X)$ of a bivariate p-power exponentially distributed random vector X satisfies the IFR-property.*

Proof According to Glaser (1980), a statistic T satisfies the IFR-property iff $\eta_T'(t) > 0$ for all $t \in \mathbb{R}$, where $\eta_T(t) = -\frac{f_T'(t)}{f_T(t)}$. Therefore, $\eta_M'(t) > 0$ for all $t \in \mathbb{R}$ and $p \geq 1$. Because of

$$\eta_m(t) = -\frac{f'_{m,g_p,p}(t)}{f_{m,g_p,p}(t)} = \frac{f'_{M,g_p,p}(-t)}{f_{M,g_p,p}(-t)} = -\eta_M(-t),$$

it is

$$\eta_m'(t) = \frac{d}{dt}\left(-\eta_M(-t)\right) = \eta_M'(-t) > 0 \quad \forall t \in \mathbb{R}\ \forall p \geq 1.$$

Hence, the minimum statistic m has the IFR-property if $p \geq 1$. □

7 Conclusion

In this paper, we demonstrate how a geometric method of deriving exact distributions of functions of random vectors, which follow an $l_{2,p}$-symmetric distribution with an arbitrary density generating funktion g, works. This method is used to obtain the cumulative distribution function of the maximum, minimum, and product statistic of $l_{2,p}$-symmetrically distributed populations. To give another example of application, the known fact that ratios of $l_{2,p}$-symmetrically distributed random variables follow a p-generalized Cauchy distribution, is proved that way. Furthermore, the probability density functions are determined in all cases and all results are numerically checked by a simulation for power-exponentially distributed populations. Finally, the increasing failure rate property is considered for extreme value statistics.

Acknowledgements The authors are grateful to the Associated Editor and a reviewer for giving valuable hints which led to improvements in the presentation of the material.

References

Adler R, Eldman R, Taqqu M (1998) A practical guide to heavy tails: Statistical techniques and applications. Birkhäuser Bosten Inc, Cambridge, MA

Anderson T (1984) An introduction to multivariate statistical analysis, 2nd edn. Wiley, New York

Arellano-Valle R, Genton M (2008) On the exact distribution of the maximum of absolutely continuous dependent random variables. Stat Probab Lett 78:27–35

Arellano-Valle R, Richter WD (2012) On skewed continuous $l_{n,p}$-symmetric distributions. Chil J Stat 3(2):193–212

Arnold B, Brockett P (1992) On distributions whose component ratios are cauchy. Am Stat 46(1):25–26

Balkema A, Embrechts P (2007) High risk scenarios and extremes: a geometric approach. European Mathematical Society Publishing House, Seminar for Applied Mathematics, Zürich

Batún-Cutz J, González-Farías G, Richter WD (2013) Maximum distributions for $l_{2,p}$-symmetric vectors are skewed $l_{1,p}$-symmetric distributions. Stat Probab Lett 83(10):2260–2268, DOI 10.1016/j.spl.2013.06.022

David H (1981) Order statistics. Wiley, New York

Fang K, Anderson T (1990) Statistical inference in elliptically contoured and related distributions. Allerton Press Inc, New York

Fang K, Zhang Y (1990) Generalized multivariate analysis. Springer, New York

Glaser R (1980) Bath tub and related failure rate characterizations. J Am Stat Assoc 75:667–672

Gumbel E (1958) Statistics of Extremes. Columbia University Press, New York

Günzel T, Richter WD, Scheutzow S, Schicker K, Venz J (2012) Geometric approach to the skewed normal distribution. J Stat Plann Inference 142(12):3209–3224, DOI 10.1016/j.jspi.2012.06.009

Gupta A, Song D (1997) l_p-norm spherical distributions. J Stat Plann Inference 60(2):241–260, DOI 10.1016/S0378-3758(96)00129-2

Gupta A, Varga T (1993) Elliptically contoured models in statistics. Kluwer Academic Publishers Norwell, Dordrecht, Boston, London

Gupta P, Gupta R (2001) Failure rate of minimum and maximum of a multivariate normal distribution. Metrika 53:39–49

Harter H (1951) On the distribution of wald's classification statistic. Ann Math Stat 22:58–67

Hyvärinen A (2007) Some extensions of score matching. Comput Stat Data Anal 51:2499–2512, DOI 10.1016/j.csda.2006.09.003

Jamalizadeh A, Balakrishnan N (2010) Distributions of order statistics and linear combinations of order statistics from an elliptical distribution as mixtures of unified skew-elliptical distributions. J Multivar Anal 101(6):1412–1427, DOI 10.1016/j.jmva.2009.12.012

Kalke S (2013) Geometrische Strukturen $l_{n,p}$-symmetrischer charakteristischer Funktionen. Dissertation, Universität Rostock

Kalke S, Richter WD (2013) Simulation of the p-generalized gaussian distribution. J Stat Comput Simulation 83(4):639–665, DOI 10.1080/00949655.2011.631187

Kalke S, Richter WD, Thauer F (2013) Linear combinations, products and ratios of simplicial or spherical variates. Commun Stat, Theory Methods 42(3):505–527, DOI 10.1080/03610926.2011.579702

Moszyńska M, Richter WD (2012) Reverse triangle inequality. antinorms and semi-antinorms. Stud Sci Math Hung 49(1):120–138, DOI 10.1556/SScMath.49.2012.1.1192

Nadarajah S (2005a) On the product and ratio of laplace and bessel random variables. J Appl Math 4:393–402

Nadarajah S (2005b) Sums, products, and ratios of non-central beta variables. Commun Stat, Theory Methods 34:89–100

Nadarajah S, Gupta A (2005) On the product and ratio for the elliptically symmetric pearson type vii distribution. Random Oper and Stoch Equ 13(2):139–146

Nadarajah S, Kotz S (2005) Linear combinations, products and ratios of t random variables. Allg Stat Arch 89(3):263–280

Nekoukhou V, Alamatsaz M (2012) A family of skew-symmetric laplace distributions. Stat Papers 53:685–696, DOI 10.1007/s00362-011-0372-7

Press S (1969) The t-ratio distribution. J Am Stat Assoc 64:242–252

Rachev S, Rüschendorf L (1991) Approximate independence of distributions on spheres and their stability properties. Ann Probab 19(3):1311–1337, DOI 10.1214/aop/1176990346

Richter WD (2007) Generalized spherical and simplicial coordinates. J Math Anal Appl 336:1187–1202, DOI 10.1016/j.jmaa.2007.03.047

Richter WD (2008a) On $l_{2,p}$-circle numbers. Lith Math J 48(2):228–234, DOI 10.1007/s10986-008-9002-z

Richter WD (2008b) On the pi-function for nonconvex $l_{2,p}$-circle discs. Lith Math J 48(3):332–338, DOI 10.1007/s10986-008-9016-6

Richter WD (2009) Continuous $l_{n,p}$-symmetric distributions. Lith Math J 49(1):93–108, DOI 10.1007/s10986-009-9030-3

Richter WD (2012) Exact distributions under non-standard model assumptions. AIP Conf Proc 1479:442–445, DOI 10.1063/1.4756160

Richter WD (2013) Geometric and stochastic representations for elliptically contoured distributions. Commun Stat, Theory Methods 42:579–602, DOI 10.1080/03610926.2011.611320

Richter WD (2014a) Geometric disintegration and star-shaped distributions. Submitted

Richter WD (2014b) Norm contoured distributions in $\mathbb{R}^2$. Submitted

Schechtman G, Zinn J (1990) On the volume of the intersection of two l_p^n balls. Proc Am Math Soc 110(1):217–224

Sinz F, Bethge M (2008) The conjoint effect of divisive normalization and orientation selectivity on redundancy reduction in natural images. Front Comput Neurosci Conference Abstract: Bernstein Symposium 2008 DOI 10.3389/conf.neuro.10.2008.01.116

Song D, Gupta A (1997) l_p-norm uniform distributions. Proc Am Math Soc 125(2):595–601

Steutel F, van Harn K (2004) Infinite divisibility of probability distributions on the real line. Marcel Dekker, New York

Subbotin M (1923) On the law of frequency errors. Mat Sb 31:296–301

Szablowski P (1998) Uniform distributions on spheres in finite dimensional l_α and their generations. J Multivar Anal 64(2):103–117, DOI 10.1006/jmva.1997.1718

Tang Q (2008) From light tail to heavy tails through multiplier. Extremes 11(4):379–391, DOI 10.1007/s10687-008-0063-5

Vázquez A, Oliviera J, Dezsö Z, Goh KI, Kondor I, Barabábsi AL (2006) Modeling bursts and heavy tails in human dynamics. Phys Rev E73 036127, DOI 10.1103/PhysRevE.73.036127, 19 pages